Title: Lignite biodegradation under conditions of acidic molasses fermentation

Author: Anna Detman, Michał Bucha, Bernd R.T. Simoneit, Damian Mielecki, Cezary Piwowarczyk, Leszek Marynowski i in.

Citation style: Detman Anna, Bucha Michał, Simoneit Bernd R.T., Mielecki Damian, Piwowarczyk Cezary, Marynowski Leszek i in. (2018). Lignite biodegradation under conditions of acidic molasses fermentation. "International Journal of Coal Geology" (Vol. 196 (2018), s. 274-287), doi 10.1016/j.coal.2018.07.015

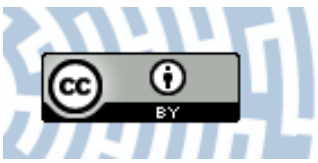

International Journal of Coal Geology 196 (2018) 274–287

Contents lists available at ScienceDirect

International Journal of Coal Geology

journal homepage: www.elsevier.com/locate/coal

Lignite biodegradation under conditions of acidic molasses fermentation

Anna Detman[a,1], Michał Bucha[b,1], Bernd R.T. Simoneit[c], Damian Mielecki[a], Cezary Piwowarczyk[a], Aleksandra Chojnacka[a], Mieczysław K. Błaszczyk[d], Mariusz Orion Jędrysek[e], Leszek Marynowski[b,*], Anna Sikora[a,*]

[a] Department of Molecular Biology, Institute of Biochemistry and Biophysics, Polish Academy of Sciences, Pawińskiego 5A, 02-106 Warsaw, Poland
[b] Faculty of Earth Sciences, University of Silesia in Katowice, Będzińska 60, 41-200 Sosnowiec, Poland
[c] Department of Chemistry, College of Science, Oregon State University, Corvallis, OR 97331, USA
[d] Faculty of Agriculture and Biology, Warsaw University of Life Sciences, Nowoursynowska 159, 02-776 Warsaw, Poland
[e] Faculty of Earth Sciences and Environmental Management, University of Wrocław, Cybulskiego 32, 50-205 Wrocław, Poland

ARTICLE INFO

Keywords:
Lignite
Acidic fermentations
Anaerobic conditions
Lignin
Microbial community
16SrRNA profiling

ABSTRACT

Lignite is difficult to degrade, thus stimulation of the autochthonous lignite microflora and introduction of additional microorganisms are required for lignite decomposition. Here, a packed bed reactor, filled with lignite samples from the Konin region (central Poland) was supplied continuously with M9 medium, supplemented with molasses (a by-product from the sugar industry), for 124 days to stimulate the autochthonous lignite microflora. Acidic fermentation of molasses was observed in the bioreactor. The simultaneous decomposition of lignite occurred under this acidic molasses fermentation condition. Our results show decay of free (non-bound) organic compounds during anaerobic lignite biodegradation. The concentrations of *n*-alkanes, *n*-alkanols, *n*-alkanoic acids, diterpenoids, triterpenoids and steroids present in non-biodegraded samples decreased significantly (some compounds to zero) during biodegradation. Interestingly, other compound classes like phenols, ketones and certain organic compounds increased. We interpret this phenomenon as a gradual decomposition of polymers, lignin and cellulose, present in the lignite. These changes resulted from microbial activity since they were not observed in pure solutions of short-chain fatty acids. The 16SrRNA profiling of the microbial community selected in the bioreactor revealed that the dominant bacteria belonged to the *Firmicutes, Actinobacteria, Proteobacteria* and *Bacteroidetes*, furthermore representatives of 16 other phyla were also found. All the known taxa of lignocellulolytic bacteria were represented in the microbial community. Synergistic relations between bacteria fermenting molasses and bacteria degrading lignite are assumed. The results confirm lignin degradation in acidic medium by bacteria under anaerobic conditions.

1. Introduction

Lignite (also known as brown coal) is a biogenic sedimentary rock formed during diagenesis and coalification of terrestrial organic matter. The primary organic constituents such as cellulose and the more recalcitrant lignin, humins or humic acids are commonly present in lignite (De Leeuw and Largeau, 1993; Fabbri et al., 2008; Fabbri et al., 2009; Grasset et al., 2010).

Lignite, a fossil fuel with the high content of lignin (a complex and heterogeneous biopolymer), is relatively difficult to biodegrade. Chemically, lignin is a mixture of polymeric compounds containing a number of aromatic rings based on phenylpropane units (Naseem et al., 2016). In addition to these, there are numerous biodegradable functional groups that facilitate the attack and cleavage of aromatic rings (Fabiańska and Kurkiewicz, 2013). The occurrence of methane of a biogenic origin in coal deposits worldwide (so called coal-bed methane) indicates that under anaerobic conditions coal can be degraded to methane by microbial activity (Batstone and Jensen, 2011; Ritter et al., 2015; Szafranek-Nakonieczna et al., 2018).

Culture-independent biogeochemical techniques were employed for molecular analyses of water that leached from coal mines or fresh raw coal samples, especially from deep-lying deposits, in Australia, USA, Canada and India. The studies showed the presence of numerous groups of bacteria (mainly representatives of *Proteobacteria, Firmicutes, Actinobacteria* and *Bacteroidetes*), whereas, surprisingly methanogenic archaeons were not always found (Barnhart et al., 2013; Barnhart et al.,

* Corresponding authors.
E-mail addresses: leszek.marynowski@us.edu.pl (L. Marynowski), annaw@ibb.waw.pl (A. Sikora).
[1] Equal contribution.

https://doi.org/10.1016/j.coal.2018.07.015
Received 10 April 2018; Received in revised form 25 July 2018; Accepted 31 July 2018
Available online 01 August 2018

2016; Li et al., 2008; Midgley et al., 2010; Penner et al., 2010; Strąpoć et al., 2008).

Based on the molecular analyses of water extracted from a coal bed in the Illinois Basin and the physiology of the microorganisms found, Strąpoć et al. (2008, 2011) proposed that lignite degradation proceeds by the following steps: (i) fragmentation of the macromolecular lignitic polycyclic aromatic carbon structure to carboxylic acids, ketones, aromatics, and aliphatics; (ii) demethylation and ring cleavage; (iii) anaerobic oxidation and fermentation of carbon components into hydrogen, carbon dioxide and acetate; and (iv) hydrogenotrophic, acetotrophic and methylotrophic methanogenesis (Strąpoć et al., 2008).

Processing coal to methanogenic substrates is the most difficult and rate-limiting step in biogenic methane production. Many efforts have been made at laboratory scales to stimulate lignite degradation by: (i) supplying additional nutrients, such as nitrogen or phosphorus-containing compounds, yeast extract, or trypticase soy broth to stimulate autochthonous microflora (Barnhart et al., 2013; Bucha et al., 2018; Opara et al., 2012), (ii) inoculation of microbes from methane-yielding environments under anaerobic conditions, like sewage waste-water sludge (Zheng et al., 2017), (iii) physical treatment such as ultrasonic wave excitation using nuclear magnetic resonance (Tang et al., 2016), or (iv) chemical treatment, e.g. with potassium permanganate (Huang et al., 2013).

Low-rank coals such as lignite are susceptible to white-rot fungal attack. *Phanerochaete chrysosporium, Trichoderma atroviride* or *Penicillium* species (e.g. *P. chrysogenum*) are recognized to solubilize coal. However, fungal decomposition of coal is an aerobic process (Shrestha et al., 2017). It has been found that detritic lignite is more susceptible to fungal attack (Hofrichter and Fakoussa, 2001), while xylites (a.k.a. fossil woods), containing abundant terpenoid compounds from residual resin that provide natural protection against microbial activity (Bechtel et al., 2007; Otto and Simoneit, 2001) are more resistant.

So far, little is known about the changes in the (macro)molecular composition of the residual organic matter of lignite after anaerobic biodegradation under laboratory conditions. Here we describe lignite degradation in a packed bed reactor (PBR) supplied with a molasses-containing medium in a continuous flow system. The microbial community of a lignite origin in the PBR was stimulated and amplified by the medium. It has been characterized by 16S rRNA profiling. The change in the lignite organic matter under this experimental approach was also analyzed.

2. Methods

2.1. Lignite sampling

Lignite samples were collected in the Konin region (central Poland). Lignites from this region were formed in the Middle Miocene (Badenian stage) and are in the early stage of diagenesis. The details regarding the geological setting as well as characterization of the lignite are published elsewhere (Fabiańska and Kurkiewicz, 2013; Widera, 2016). Currently, lignite from the Konin location is exploited by the company PAK Kopalnia Węgla Brunatnego Konin S.A. from three open pits (Drzewce, Jóźwin IIB, Tomisławice). The lignite for this study was collected from the Jóźwin IIB open pit (52° 24.781′N, 18° 10.150′E) at a freshly exposed wall with lignite beds. The collection (ca. 1 kg) represents an equal mixture of detritic, detroxylitic and xylodetritic lignite, according to the (Widera, 2016) classification.

2.2. Experimental set-up for lignite treatment

The lignite described above was put into a 3 l-packed bed reactor (PBR) made of plexiglass. The bioreactor was filled with the sterile cultivation medium containing molasses at a concentration of 30.1 ± 1.7 g COD/L (COD, chemical oxygen demand). The cultivation medium was a modified M9 medium (Miller, 1972), where $MgSO_4$ was replaced by $MgCl_2$ (190 mg/L), no glucose was added, and pH = 7. The molasses came from the Dobrzelin Sugar Factory (Polish Sugar Company "Polski Cukier", Poland). The medium was sterilized by boiling and saturated with a stream of pure N_2 (Air Products, Poland). Additionally, another 50 g lignite sample was incubated at 28 °C in the same cultivation medium containing molasses under anaerobic conditions (Coy Laboratory Products, USA) for 6 days and finally added to the bioreactor. Thus, the lignite acted as a solid phase and a source of microorganisms in the PBR; molasses was a selecting/stimulating factor for autochthonous microorganisms. The bioreactor was incubated at room temperature (23–25 °C) for 5 days. The medium (with the same contents) flow was then switched on and the experimental system was maintained for 124 days at room temperature (23–25 °C). The hydraulic retention time (HRT) was 120 h, until the 43rd day of the experiment and from the 44th day the HRT was 30 h. The working volume of the bioreactor was 2.5 L. After the 79th day of cultivation the supplied medium was diluted 10 times and containing molasses at a concentration of 0.7 g COD/L. The HRT was increased to 120 h and the experimental system maintained for further 60 days at room temperature (23–25 °C). Samples taken from the bioreactor on the 79th experiment day were subjected to molecular analyses. Additional control tests with lignite treated with organic acid solutions, but without molasses, were carried out. The details are presented in the Supplementary file 3.

2.3. Analyses of effluent from the PBR during the experiment

The pH of the effluent from the PBR was measured using a standard pH meter (Elmetron model CP-502). COD of the effluent was determined using a Nanocolor COD 1500 kit (Machery-Nagel) according to ISO 1575:2002. The total rate of gas production was measured using a MGC-1 MilliGascounter (Ritter). The composition of the fermentation gas was analyzed using a HPR20 mass spectrometer (Hiden, England) with QGA version 1.37. The concentration of short-chain fatty acids in the effluent was analyzed by HPLC with photometric detection (Waters HPLC system with Waters 2996 – Photodiode Array Detector, using a 300 × 7.8 mm Aminex HPX-87H column with guard column). The HPLC conditions were as described previously (Chojnacka et al., 2011).

The concentration of sulphide (S^{2-}) in the cultivation medium and the effluent was determined using a Nanocolor SULFID 3 kit (Machery-Nagel) according to the method DIN 38405-D26/27.

Effluents were centrifuged (7000 rcf) before the analyses to remove microbial cells and debris. The mean values ± SD (standard deviation) were calculated for the data from all sample analyses.

2.4. Total organic carbon content determination

Total organic carbon (TOC) was determined using an Eltra CS-500 IR-analyzer. The TOC was measured by using an infrared cell detector for CO_2, which evolved from the combustion of organic matter under an oxygen atmosphere. This lignite does not contain carbonates. The instrument was calibrated utilizing the Eltra standards.

2.5. Holocellulose and lignin content determination

The holocellulose (cellulose and hemicelluloses) content (%) was quantified with using modified TAPPI T-222 method applied from the paper industry. In this method holocellulose is hydrolized by reaction with 72% sulfuric acid. In the case of lignite the residue after such treatment contains lignin (also known as Klason lignin), mineral matter as well as humins. The percentage of decomposed organic matter is in this case equal to the holocellulose content and can be calculated according to Eq. (1).

$$\text{Holocellulose (\%)} = \text{A (100\%)} - \text{B (\%)} - \text{C (\%)}, \text{ where: A = sample, B = residue after treatment, and C = ash} \quad (1)$$

The determination of holocellulose content (%) started with extraction of the lignite and lignite after biodegradation with a mixture of dichloromethane (DCM) and methanol (1:1) and drying in the oven at 105 °C for 90 min before the reaction with sulfuric acid. Dry samples (1 g) were treated with cold (10 °C) 72% sulfuric acid for 2 h at room temperature. Next the solution with sample and sulfuric acid was diluted to 3% and boiled for 4 h in a round bottom flask connected to a reflux condenser. The residue after chemical treatment was rinsed several times with hot distilled water to obtain a neutral pH. At the end, the residue was dried in oven at 105 °C and weighed. Analyses were carried out in duplicate with a precision error of < 1.0%. The ash content in lignite was determined by combustion at 810 °C in a muffle furnace (Marynowski et al., 2018).

2.6. Extraction, separation and derivatization

Prior to the molecular analyses a representative sample of the source lignite (~1 kg) used in the bioreactors was crushed in a mill to obtain powder with particle sizes < 0.5 mm. The biodegraded lignite was collected together with the fermentation solution. After removing the water from the sample by lyophilization, it was crushed in the same way.

Powdered samples (ca. 5–10 g) were extracted using a DCM/methanol mixture (1:1 v:v) with an accelerated Dionex ASE 350 solvent extractor. Extract aliquots were separated into aliphatic, aromatic and polar fractions by modified column chromatography (Bastow et al., 2007). Silica-gel was activated at 110 °C for 24 h. The eluents used for collection of the organic fractions were: *n*-pentane (aliphatic), *n*-pentane and DCM (7:3, aromatic), and DCM and methanol (1:1, polar). Aliquots of the polar fractions were reacted to trimethylsilyl (TMS) derivatives with *N*,*O*-bis-(trimethylsilyl)trifluoroacetamide (BSTFA), 1% trimethylchlorosilane, and 10μL of pyridine for 3 h at 70 °C. Prior to analysis these derivatized mixtures were dried and dissolved in *n*-hexane. The extracts of the source lignite and lignite after biodegradation were analyzed in triplicate.

Two blank samples (silica gel and Al_2O_3) were analyzed using the same procedure (including extraction and separation on columns). Trace amounts of phthalates, *n*-alkanoic acids, *n*-alkanols and squalene were found. Molasses was derivatized as above and analyzed, and only sucrose was present.

2.7. Gas chromatography - mass spectrometry (GC–MS)

GC–MS analyses were carried out with an Agilent Technologies 7890A gas chromatograph and Agilent 5975C Network mass spectrometer with Triple-Axis Detector (MSD) at the Faculty of Earth Sciences, Sosnowiec, Poland. Helium was used as a carrier gas. Separation was obtained on J&W HP5-MS (60 m × 0.32 mm i.d., 0.25 μm film thickness) fused silica capillary column coated with a chemically bonded phase (5% phenyl, 95% methylsiloxane). The GC oven temperature was programmed from 45 °C (1 min) to 100 °C at 20 °C/min, then to 300 °C (hold 60 min) at 3 °C/min, with a solvent delay of 10 min.

The GC column outlet was connected directly to the ion source of the MSD. The GC–MS interface was set at 280 °C, while the ion source and the quadrupole analyzer were set at 230 and 150 °C, respectively. Mass spectra were recorded from 45 to 550 da (0–40 min) and 50–700 da (> 40 min). The MS was operated in the electron impact mode, with an ionization energy of 70 eV. An Agilent Technologies MSD ChemStation E.02.01.1177 and the Wiley Registry of Mass Spectral Data (9th edition) software were used for data collection and mass spectra processing. Mono- and disaccharides were identified based on comparison of mass spectra and retention times with those of standards. The following standards were used: D-glucose (Sigma-Aldrich), mannitol (Sigma-Aldrich), erythritol (Sigma-Aldrich), inositol (Sigma-Aldrich), sucrose (Sigma-Aldrich). Hexadecane-1-d, phenanthrene-d_{10} and ethyl vanillin were used as internal standards (Sigma-Aldrich).

2.8. Total DNA isolation and 16SrRNA profiling

Total DNA from the microbial community stimulated and selected by molasses in the PBR was isolated from samples on the 79th day of the experiment. DNA was extracted and purified using a PowerSoil DNA isolation kit (MoBio Laboratories, Carlsbad, CA) according to the manufacturer's protocol with some modifications. Six 0.3-g samples of the lignite were placed into six bead tubes for extraction. These tubes were incubated at 65 °C for 20 min and then shaken horizontally in a MoBio vortex adapter for 20 min at maximum speed. The remaining steps were performed as directed by the manufacturer. The final samples of DNA extracted from the five replicates were pooled and stored at −20 °C. The total mass of purified DNA was 57 μg, respectively.

Using the total DNA isolated from the microbial community as template, the hypervariable V3-V4 region of the 16S rRNA gene was amplified by PCR. The universal primers 341F and 785R were employed for the simultaneous detection of *Bacteria* and *Archaea* (Takahashi et al., 2014). PCR was performed using the Q5 Hot Start High-Fidelity Master Mix (NEB) according to the manufacturer's instructions. Sequencing of the amplified V3-V4 region libraries was performed using a MiSeq next generation sequencer (Illumina) with 2 × 250 nt paired-end technology (PE), and the v2 Illumina kit. Automatic analysis of the data to determine the composition of the microbial communities was carried out using 16S Metagenomics software available on the BaseSpace server (Illumina). This analysis consisted of three stages: (i) automatic demultiplexing of the samples, (ii) generation of fastq files containing the raw reads, and (iii) classification of the reads into taxonomic categories.

The 16S Metagenomics Protocol classifies the reads to species level based on the Greengenes v13_5 reference database, modified by Illumina. This modification comprises filtering out the following sequences: (i) of < 1250 base pairs (bp) in length; (ii) containing > 50 degenerate bases (M, R, W, S, Y, K, V, H, D, B, N); and (iii) those incompletely classified, i.e. not to the level of genus or species. Molecular analysis of the microbial communities was performed by the Genomed Joint-Stock Company (Warsaw, Poland).

Two diversity indices were calculated: the Shannon-Wiener index, according to the equation $H' = -\sum_{i=1}^{R} pi \ln pi$ (where *pi* is the proportion of the *i*th element), and True Diversity being ${}^1D = e^{H'}$ (Shannon, 1948; Tuomisto, 2010).

All raw sequences generated in this study have been deposited in NCBI databases with the following accession numbers: BioProject – PRJNA381161; BioSample – SAMN06671879; and SRA – SRP102779.

3. Results

3.1. Performance of the experimental set-up for lignite treatment in PBR reactor and macroscopic changes in the lignite structure

Changes typical for acidic fermentation of molasses were observed during the first 5 days of the lignite incubation with the medium, i.e. intensive fermentation gas production and acidification of the culture fluids. The fermentation was maintained continuously after switching on the medium flow. Tables 1 and 2 present the data describing the progression of the experiment.

Analysis of the fermentation gas and effluents from the bioreactor revealed that the molasses stimulated the development of hydrogen and lactic acid producing bacteria. The fermentation gas was composed of carbon dioxide and hydrogen, with traces of hydrogen sulfide, but no methane. This is a typical composition for hydrogen fermentations. These conditions are inhibitory for methanogenesis. Fermentation gas was produced more intensively after decreasing the HRT value from

Table 1
Progression of the experiment of lignite degradation.

Experimental conditions	30 g COD molasses/L HRT 120 h, 33rd–43rd day of experiment	30 g COD molasses/L HRT 30 h, 60th–70th day of experiment	0.7 g COD molasses/L HRT 120 h, 110th–120th day of experiment
Parameters			
pH of the effluent	4.8–5.1, $n = 5$	4.6–4.7, n = 5	4.6–5.5, n = 5
COD of the effluent (g/L)	22.1–25.6, n = 5	26.2–27.1, $n = 3$	1.2–1.6, $n = 9$
Sulfate concentration (mg/L)[a]	69, n = 3	54, n = 3	< 10, n = 3
Fermentation gas production (cm^3/min)	1.1–2.2, $n = 6$	4.2–4.5, n = 3	Not measurable
Composition of fermentation gas (%)			
Hydrogen	21–40, n = 5	25–35, n = 3	–
Carbon dioxide	60–79, n = 5	65–75, n = 3	–
Methane	0, n = 5	0, n = 3	–
Hydrogen sulfide	0.1, n = 5	0.1, n = 3	–

[a] The sulfate concentration in the molasses containing medium was 73 mg/L and < 10 mg/L, respectively, at molasses concentrations of 30 g COD/L and 0.7 g COD/L.

Table 2
Compositions of the substrate and effluent from the PBR bioreactor packed with lignite. The data are for replicates.

Component	Molasses containing medium	Day of experiment			
		42	49	51	56
Ethanol [g/100 g]	0.01	0.02	0.06	0.05	0.20
Sucrose[g/L]	20.40	0.11	0.18	0.18	0.31
Glucose [g/L]	0.14	< 0.01	< 0.01	< 0.01	< 0.01
Fructose [g/L]	0.17	0.03	0.12	0.10	0.13
Lactic acid [g/L]	1.08	0.11	0.77	0.38	5.30
Formic acid [g/L]	0.84	0.13	< 0.001	< 0.001	< 0.001
Acetic acid [g/L]	0.72	1.14	1.36	1.03	2.40
Propionic acid [g/L]	0.47	1.12	1.20	0.91	0.94
Butyric acid [g/L]	0.14	8.16	8.05	7.20	5.36

120 to 30 h. A sudden drop in fermentation gas production was observed when the concentration of molasses in the medium was decreased from 30 to 0.7 g COD/L.

The pH values of the effluent were in the range 4.6–5.5 during the experiment. At the higher molasses concentration (30 g COD/L) in the bioreactor, the COD value of the effluent was lower than the substrate. Interestingly, the COD value of the effluent was higher than the COD of the supplied medium (at 0.7 g COD/L), suggesting that the effluent contained additional compounds coming from lignite degradation.

The effluents from the bioreactor contained short chain carboxylic acids and ethanol (Table 2), typical products of acidic fermentations. Sucrose was derived at least partially from unfermented molasses. The sulfate concentrations in both the supplied medium and the effluent were comparable (Table 1).

At the same time significant changes were observed in the macroscopic lignite structure. The highly heterogeneous lignite structure changed to a solid mud and sludge. Interestingly, most of the xylite fibers were degraded. Fig. 1 shows the macroscopic changes of lignite in the PBR bioreactor during the experiment, and the lignite on the first and last days of the experiment.

In parallel experiments using PBR bioreactors packed with lignite, where the M9 medium was supplemented with yeast extract, propylbenzene (200 mg/L), and acetate or glucose (each at a concentration of 200 mg/L), no changes in the lignite structure were observed. The macroscopic appearance of the lignite in the bioreactor was the same after 130 days of the experiment (data not shown) as at the beginning.

3.2. Composition of lignite extracts before and after biodegradation

The total organic carbon content (TOC) of the lignite samples was in the range of 49.6 to 60.7%. The total sulfur content (TS) varied from 1.5 to 5.6%. The ash content ranged from 3.8 to 15.7%. The holocellulose contents in lignite used as substrate and after biodegradation were 7.0 and 6.1%, respectively. The lignin contents (considered as the residue after treatment) in the substrate lignite and after biodegradation were equal at 75.0% and 76.1%, respectively. The ratio lignin:cellulose increased from 11 to 13 after biodegradation, when compared to the substrate lignite.

The concentrations of compound classes from the in fresh (IBB1B) and biodegraded (F1) lignite extracts are given in Table 3 and the detailed compositions are found in Table 4. Our results show a significant decrease of some compound groups after biodegradation, while concentrations of others increase significantly (Table 3).

The *n*-alkane concentration decreases almost twice, but without a significant change in their high molecular weight, odd-numbered predominance (Fig. 2). The aliphatic diterpenoids decreased considerably (Table 3), mainly due to the loss of 13β-methylpodocarpane, from 3.98 to 0.19 μg/g TOC (Table 4; Fig. 2). Other aliphatic diterpenoids were also preferentially biodegraded, although 16α(H)-phyllocladane seems to be more resistant (Table 4; Fig. 2). In contrast the aliphatic triterpenoid and hopanoid concentrations changed only slightly (Tables 3 and 4). The aromatic diterpenoid and triterpenoid concentrations decreased significantly, but like the *n*-alkanes, these compounds were degraded proportionally, not changing their distributions (Fig. 3). The most abundant compound in the aromatic fraction of biodegraded lignite is acetophenone (> 1 μg/g TOC; Table 4), and it was not detected in the fresh lignite (Fig. 3).

The most severe changes were observed for the polar compounds after biodegradation. Although the concentrations of the carboxylic acids are similar, their composition has undergone significant modification during biodegradation. The total *n*-alkanoic acids decreased from 21 to 16 μg/g TOC. Also, the concentrations of 1,25-pentacosanedioic and 1,27-heptacosanedioic acids decreased about twice (Table 4). On the other hand, the lactic, succinic and piperidine-2-carboxylic acid concentrations increased from trace to 5.8, 3.2 and 0.2 μg/g TOC, respectively (Fig. 4). However, lactic acid and possibly also succinic acid are fermentation products from molasses. The concentrations of *n*-alcohols, tocopherols, and all polar diterpenoids decreased (Tables 3 and 4). 6,7-Dehydroferruginol, among others decreased significantly from 1.1 to 0.4 μg/g TOC (Table 4; Fig. 4), and for imbricatolic acid, the concentration decrease was minimal (0.16 vs. 0.14 μg/g TOC). Polar triterpenoids had diverse, but insignificant decreases depending on the particular compound (Table 4). Phenols and saccharides are two compound classes, which increased significantly in concentrations. In the case of phenols both concentration increased and distribution changed (Table 4; Fig. 5). The dominant compounds the lignite, like benzoic acid, 4-hydroxybenzaldehyde, and vanillic acid increased after biodegradation (Table 4), but others absent in the lignite, like 3-phenylpropanoic and phloretic acids, became dominant (Fig. 5; Table 4). Saccharides were essentially absent in the fresh lignite, but appeared in the extract after biodegradation (Fig. 6; Table 4). Erythritol and glucose were major with

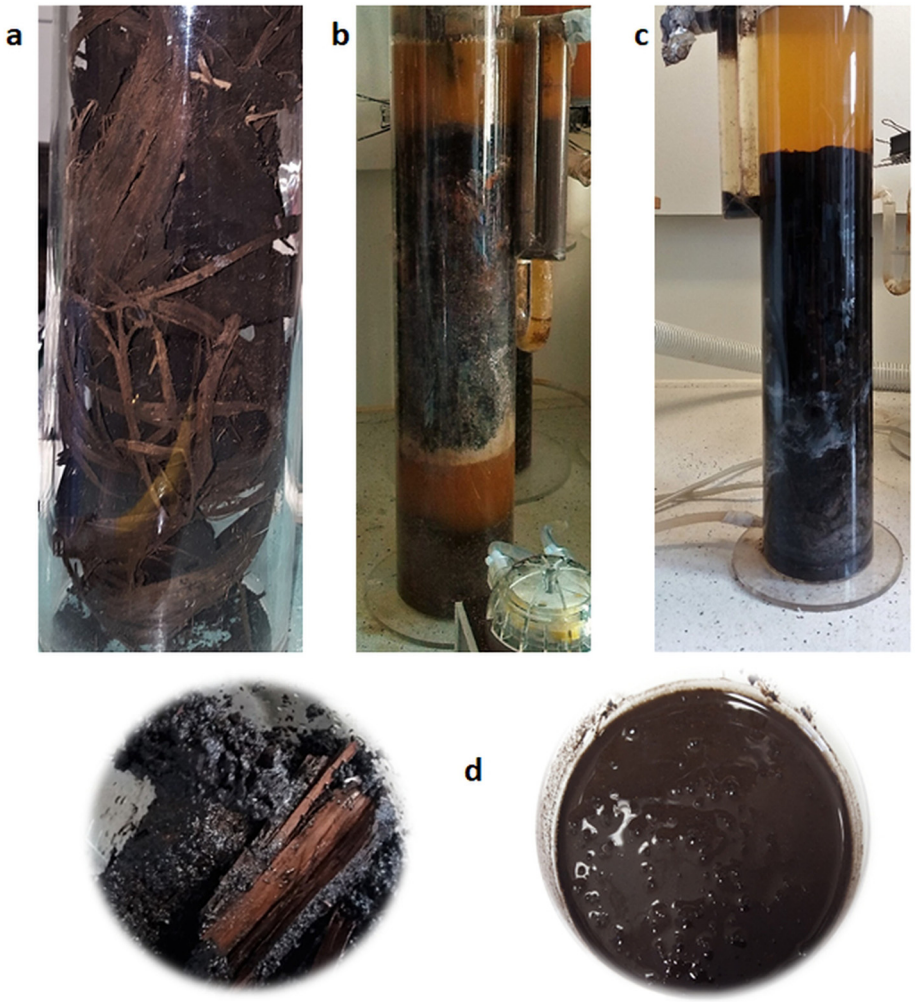

Fig. 1. Macroscopic changes in the lignite structure in the PBR bioreactor supplied with molasses-containing medium in the 1st (a), 61st (b), 124th (c) day of the experiment; and samples (on Petri dishes) taken out from the bioreactor at the end of the experiment (d). The photos show the bioreactor and samples of lignite on the respective day of the experiment.

Table 3
Concentrations of compound classes present in extracts of the fresh (IBB1B) and biodegraded (F1) lignite.

Compound classes	IBB1B [μg/g TOC]	F1 [μg/g TOC]
Alkanes	1.19	0.72
Alkanols	12.30	8.48
Alkanoic acids	24.76	26.93
Phenols and ketones	0.22	7.19
Saccharides	0.00	1.17
Aliphatic diterpenoids	4.82	0.38
Aromatic diterpenoids	0.05	0.02
Polar diterpenoids	3.40	1.17
Aliphatic triterpenoids	0.08	0.07
Aromatic triterpenoids	7.23	2.98
Polar triterpenoids	12.04	8.90
Steroids	1.43	0.80
Hopanoids	1.15	1.01

minor ribonic acid, mannitol, inositol and sucrose (Fig. 6), but their concentrations did not exceed 0.5 μg/g TOC.

3.3. Biodiversity of the lignite microbial community stimulated by molasses

The 16S rRNA gene fragment libraries amplified from DNA isolated from the lignite microbial community stimulated by molasses were sequenced. The total number of reads was 268 126 and 100% of them passed the quality filtering.

Diversity indices were calculated for the analyzed microbial community. The Shannon-Wiener index was 2.89 at the species level, and 1.74 at the genus level. The respective True Diversity index value was 18.05 at the species level, and 5.69 at the genus level. These diversity indices indicate that the microbial community is moderately rich in species but diversity drops for genera.

The 268,097 reads were assigned to *Bacteria* while 29 remained unclassified at the Kingdom level. No reads were assigned to *Archaea*.

The domain *Bacteria* was represented mainly by *Firmicutes* (68.8%), *Bacteroidetes* (19.1%), *Actinobacteria* (6.9%) and *Gammaproteobacteria* (4.8%). However, some genera belonging to those phyla predominated and the others were minor (< 10 reads). The representatives of *Alpha-*, *Beta-*, *Delta-* and *Epsilonproteobacteria* were also in the minority (0.034%, 0.006%, 0.016%, 0.003%, respectively). Other minor reads belonged to *Chloroflexi* (0.005%), *Cyanobacteria* (0.005%), *Planctomycetes* (0.002%), *Verrucomicrobia* (0.002%), *Synergistetes* (0.002%), *Tenericutes* (0.001%), *Nitrospirae* (0.001%), *Calditthrix* (0.0007%), *Thermi* (0.0007%), *Spirochaetes* (0.0004%), *Acidobacteria* (0.0004%), *Chlamydiae* (0.0004%), *Chlorobi* (0.0004%), *Thermodesulfobacteria* (0.0004%) and *Fusobacteria* (0.0007%). A summary of the taxonomic assignments is listed in Table 5 and detailed assignments are given in Supplementary files 1 and 2.

Table 4
Concentrations of major compounds identified in extracts of the fresh (IBB1B) and biodegraded (F1) lignite.

Compound	MW	Composition	IBB1B [μg/g TOC]	F1 [μg/g TOC]
Aliphatic lipids				
Alkanes				
n-Tricosane	324	$C_{23}H_{48}$	0.024	0.019
n-Tetracosane	338	$C_{24}H_{50}$	0.013	0.012
n-Pentacosane	352	$C_{25}H_{52}$	0.049	0.046
n-Hexacosane	366	$C_{26}H_{54}$	0.019	0.015
n-Heptacosane	380	$C_{27}H_{56}$	0.135	0.088
n-Octacosane	394	$C_{28}H_{58}$	0.029	0.019
n-Nonacosane	408	$C_{29}H_{60}$	0.458	0.265
n-Triacontane	422	$C_{30}H_{62}$	0.031	0.018
n-Hentriacontane	436	$C_{31}H_{64}$	0.436	0.241
Alcohols				
n-Docosanol	326	$C_{22}H_{46}O$	0.740	0.362
n-Tetracosanol	354	$C_{24}H_{50}O$	3.238	2.306
n-Hexacosanol	382	$C_{26}H_{54}O$	3.339	2.265
n-Octacosanol	410	$C_{28}H_{58}O$	2.566	1.365
n-Triacontanol	438	$C_{30}H_{62}O$	2.369	1.088
2,3-Butanediol	90	$C_4H_{10}O_2$	0	0.982
Glycerol	92	$C_3H_8O_3$	0.053	0.113
Carboxylic acids				
n-Hexadecanoic acid	256	$C_{16}H_{32}O_2$	0.247	2.288
n-Octadeca-9,12-dienoic acid	280	$C_{18}H_{32}O_2$	0.046	0.249
n-Octadecanoic acid	284	$C_{18}H_{36}O_2$	0.088	0.466
n-Tetracosanoic acid	368	$C_{24}H_{48}O_2$	1.618	0.873
n-Hexacosanoic acid	396	$C_{26}H_{52}O_2$	6.691	4.518
n-Octacosanoic acid	424	$C_{28}H_{56}O_2$	7.021	4.514
n-Triacontanoic acid	452	$C_{30}H_{60}O_2$	5.302	3.005
Lactic acid	90	$C_3H_6O_3$	0.075	5.767
Succinic acid	118	$C_4H_6O_4$	0.010	3.163
1,25-Pentacosanedioic acid	412	$C_{25}H_{48}O_4$	2.148	1.238
1,27-Heptacosanedioic acid	440	$C_{27}H_{52}O_4$	1.518	0.652
Piperidine-2-carboxylic acid	273	$C_{12}H_{27}NO_2$	0	0.199
Isoprenoids				
Squalane	422	$C_{30}H_{62}$	0.020	0.010
β-Tocopherol	416	$C_{28}H_{48}O_2$	0.237	0.142
α-Tocopherol	430	$C_{29}H_{50}O_2$	0.613	0.430
Phenols and ketones (lignin degradation products)				
Acetophenone	120	C_8H_8O	0	1.031
2-Phenylethanol	122	$C_8H_{10}O$	0	0.013
Benzoic acid	122	$C_7H_6O_2$	0.037	0.096
4-Hydroxybenzaldehyde	122	$C_7H_6O_2$	0.010	0.035
3-Phenylpropanoic (hydrocinnamic) acid	150	$C_9H_{10}O_2$	0.001	1.667
2-Hydroxybenzoic acid	138	$C_7H_6O_3$	0.006	0.091
Vanillin	152	$C_8H_8O_3$	0.015	0
3-Hydroxybenzoic acid	138	$C_7H_6O_3$	0.016	0.003
Tyrosol	138	$C_8H_{10}O_2$	0.001	0.082
4-Hydroxybenzoic acid	138	$C_7H_6O_3$	0.039	0.204
4-Hydroxyphenylacetic acid	152	$C_8H_8O_3$	0	0.096
Phloretic acid	166	$C_9H_{10}O_3$	0.007	2.493
Vanillic acid	168	$C_8H_8O_4$	0.051	0.149
Terephthalic acid	166	$C_8H_6O_4$	0.022	0.743
p-Coumaric acid	164	$C_9H_8O_3$	0	0.182
Syringic acid	198	$C_9H_{10}O_5$	0.011	0.001
3,4-Dihydroxy-hydrocinnamic acid	182	$C_9H_{10}O_4$	0	0.208
Ferulic acid	194	$C_{10}H_{10}O_4$	0	0.106
Saccharides				
Erythritol	122	$C_4H_{10}O_4$	0	0.314
Ribonic acid	165	$C_5H_9O_6$	0	0.408
α-Glucose	180	$C_6H_{12}O_6$	0	0.111
Mannitol	182	$C_6H_{14}O_6$	0	0.174
β-Glucose	180	$C_6H_{12}O_6$	0	0.070
Inositol	180	$C_6H_{12}O_6$	0	0.021
Sucrose	342	$C_{12}H_{22}O_{11}$	0	0.068
Terpenoids				
Sesquiterpenoids				
α-Cedrane	204	$C_{15}H_{24}$	0.094	0.085
Calamene	202	$C_{15}H_{22}$	0.046	0.042

(*continued on next page*)

Table 4 (*continued*)

Compound	MW	Composition	IBB1B [μg/g TOC]	F1 [μg/g TOC]
Diterpenoids				
Aliphatic hydrocarbons				
13*β*-Methylpodocarpane	248	$C_{18}H_{32}$	3.983	0.189
13-Methylpodocarp-13-ene	246	$C_{18}H_{30}$	0.063	0.009
13*α*-Methylpodocarpane	248	$C_{18}H_{32}$	0.061	0.007
Fichtelite	262	$C_{19}H_{34}$	0.135	0.044
Isopimarane	276	$C_{20}H_{36}$	0.448	0.067
Abietane	276	$C_{20}H_{36}$	0.061	0.016
16*α*(H)-Phyllocladane	274	$C_{20}H_{34}$	0.067	0.047
Aromatic hydrocarbons				
Dehydroabietane	270	$C_{20}H_{30}$	0.010	0.001
Simonellite	252	$C_{19}H_{24}$	0.012	0.004
Retene	234	$C_{18}H_{18}$	0.021	0.011
19-Norabieta-8,11,13-triene	256	$C_{19}H_{28}$	0.005	0.001
18-Norabieta-8,11,13-triene	256	$C_{19}H_{28}$	0.007	0.001
Polar compounds				
12-Hydroxysimonellite	268	$C_{19}H_{24}O$	0.197	0.065
6,7-Dehydroferruginol	284	$C_{20}H_{28}O$	1.121	0.372
Ferruginol	286	$C_{20}H_{30}O$	0.376	0.164
Dehydroabietic acid	300	$C_{20}H_{28}O_2$	0.308	0.124
Abietic acid	302	$C_{20}H_{30}O_2$	0.076	0.053
Sugiol	300	$C_{20}H_{28}O_2$	0.697	0.188
Levopimaric acid	302	$C_{20}H_{30}O_2$	0.212	0.031
Labdan-15-oic acid	308	$C_{20}H_{36}O_2$	0.249	0.030
Imbricatolic acid	322	$C_{26}H_{50}O_3$	0.168	0.141
Triterpenoids				
Aliphatic hydrocarbons				
Des-A-oleana-5(10),12-diene	326	$C_{24}H_{38}$	0.020	0.016
Olean-12-ene	410	$C_{30}H_{50}$	0.003	0.002
Fern-8-ene	410	$C_{30}H_{50}$	0.060	0.054
Aromatic hydrocarbons				
3,4,7-Trimethyloctahydrochrysene	278	$C_{21}H_{26}$	0.027	0.029
3,3,7-Trimethyloctahydrochrysene	278	$C_{21}H_{26}$	0.046	0.021
Des-A-26,27-bisnoroleana-5,7,9,11,13-pentaene	292	$C_{22}H_{28}$	0.031	0.015
Des-A-26,27-bisnorursana-5,7,9,11,13-pentaene	292	$C_{22}H_{28}$	0.007	0.003
Des-A-26,27-bisnorlupana-5,7,9,11,13-pentaene	292	$C_{22}H_{28}$	0.003	0.003
3,3,7-Trimethyl-1,2,3,4-tetrahydrochrysene	274	$C_{21}H_{22}$	0.046	0.020
23,25-Bisnoroleana-1,3,5(10),12-tetraene	376	$C_{28}H_{40}$	1.471	0.857
23,25-Bisnorursana-1,3,5(10),12-tetraene	376	$C_{28}H_{40}$	0.238	0.132
23,25-Bisnorlupanatriene	378	$C_{28}H_{42}$	0.088	0.048
2,2,4a,9-Tetramethyloctahydropicene	342	$C_{26}H_{30}$	0.477	0.171
1,2,4a,9-Tetramethyloctahydropicene	342	$C_{26}H_{30}$	0.132	0.038
1,2,9-Trimethyl-1,2,3,4-tetrahydropicene	324	$C_{25}H_{24}$	2.254	1.056
2,2,9-Trimethyl-1,2,3,4-tetrahydropicene	324	$C_{25}H_{24}$	2.254	0.539
1,2,9-Trimethyl-1,2-dihydropicene	322	$C_{25}H_{22}$	0.158	0.052
Polar compounds				
Lupeol	426	$C_{30}H_{50}O$	0.398	0.189
Friedelin	426	$C_{30}H_{50}O$	1.084	0.549
β-Amyrone	424	$C_{30}H_{48}O$	0.410	0.403
α-Amyrone	424	$C_{30}H_{48}O$	0.174	0.214
β-Amyrin	426	$C_{30}H_{50}O$	2.440	1.247
α-Amyrin	426	$C_{30}H_{50}O$	0.499	0.372
Oleanolic acid	456	$C_{30}H_{48}O_3$	1.494	1.377
Ursolic acid	456	$C_{30}H_{48}O_3$	5.541	4.551
Steroids				
4-Stigmastene	398	$C_{29}H_{50}$	0.099	0.062
5-Stigmastene	398	$C_{29}H_{50}$	0.067	0.044
1-Methyl-24-ethyl-19-norholesta-5,7,9-triene	394	$C_{29}H_{46}$	0.038	0.014
Sitosterol	414	$C_{29}H_{50}O$	1.222	0.680
Hopanoids				
Hop-17(21)-ene	410	$C_{30}H_{50}$	0.307	0.329
17*β*(H),21*β*(H)-29-Norhopane	398	$C_{29}H_{50}$	0.064	0.047
17*β*(H),21*β*(H)-30-Hopane	412	$C_{30}H_{52}$	0.065	0.063
17*α*(H),21*β*(H)-31-Homohopane-22R	426	$C_{31}H_{54}$	0.610	0.489
17*β*(H),21*β*(H)-31-Homohopane-22R	426	$C_{31}H_{54}$	0.100	0.080

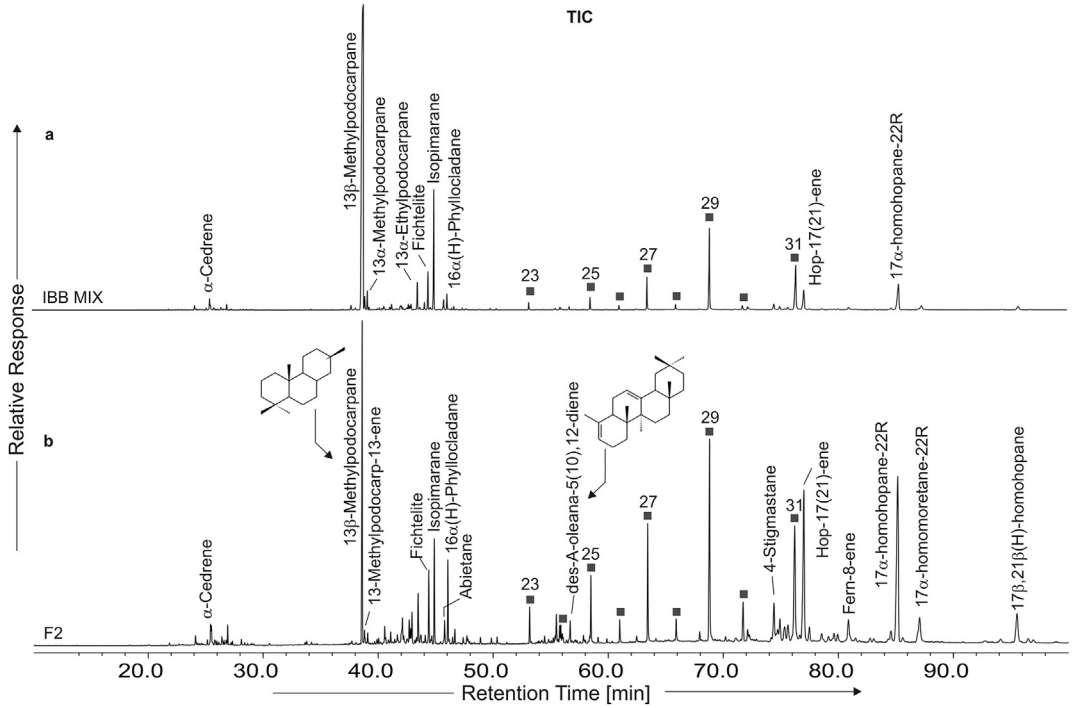

Fig. 2. Total ion current (TIC) traces of aliphatic hydrocarbon fractions from non-biodegraded (a) and biodegraded (b) lignite. The *n*-alkanes are marked by squares. Numbers over the peaks represent the carbon-number of particular homologues.

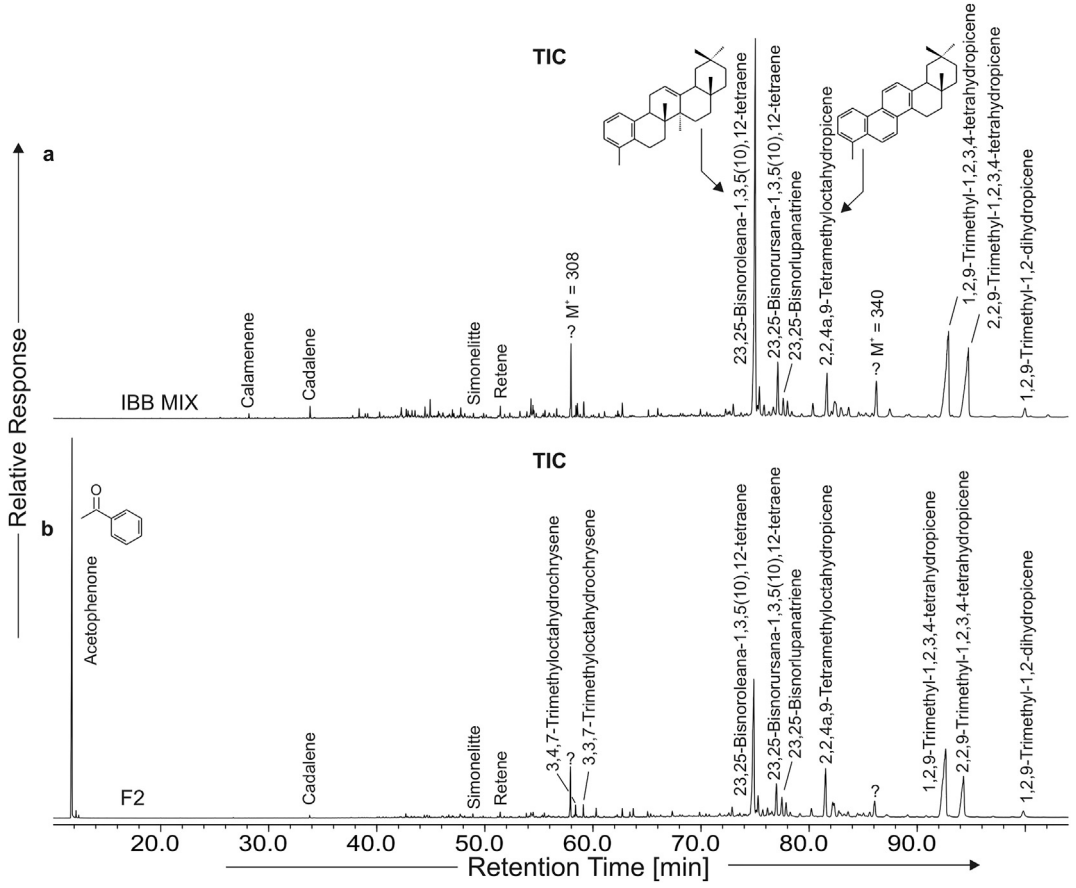

Fig. 3. TIC traces of aromatic fraction of the non-biodegraded (a) and biodegraded (b) lignite. Note the presence of acetophenone as the dominant compound in biodegraded lignite.

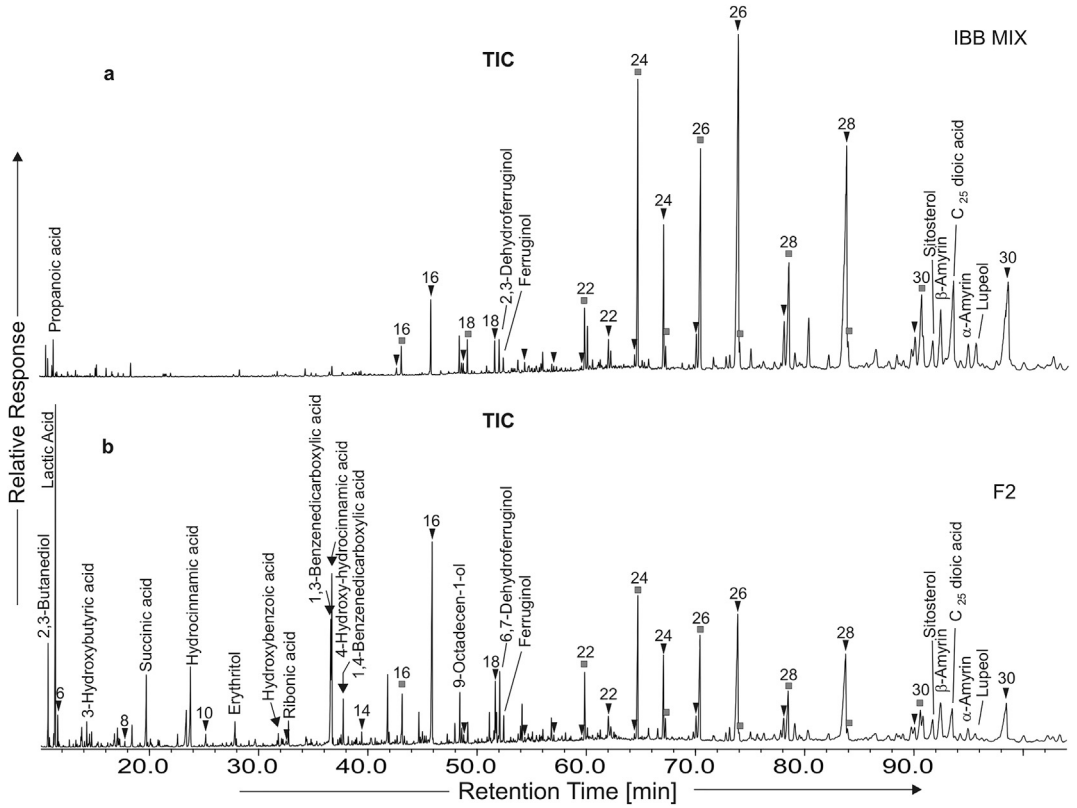

Fig. 4. TIC traces of the polar compound fraction from non-biodegraded (a) and biodegraded (b) lignite. The *n*-alkanoic acids are marked by triangles and *n*-alkanols are marked by squares. Numbers over the peaks represent the carbon-number of particular homologues.

4. Discussion

Lignite is a refractory material, otherwise it would be decomposed as easily as modern plant organic matter in the natural environment. Thus, stimulation of autochthonous microflora in lignite and introduction of additional microorganisms are required for lignite degradation (Robbins et al., 2016; Strąpoć et al., 2011).

The idea for the experimental system used in this study comes from that described previously for hydrogen-producing microbial community processing of molasses in a continuous system PBR (Chojnacka et al., 2011). Here, the molasses-containing medium was used to stimulate autochthonous microflora in lignite for degradation of lignite to a mixture of various compounds after depolymerisation and partial fermentation of monomers. According to the scheme of lignite degradation proposed by Strąpoć et al. (2008, 2011) the observed processes are mostly limited to the first stage, i.e. fragmentation of the macromolecular lignitic polycyclic aromatic carbon structure to carboxylic acids, ketones as well as aromatic, and aliphatic hydrocarbons. These processes resulted from microbial activity since they were not observed in pure solutions of short-chain fatty acids (for details see the Supplementary file 3).

4.1. Biodegradation of polymers

So far, little has been published about the changes in lignite organic matter caused by anaerobic biodegradation under laboratory conditions. It is therefore important to observe the changes in the (macro)molecular composition of the residual lignite organic matter, and to identify the products of polymer degradation in the fermentation solution.

Our results show intense decay of free (non-bound) organic compounds (mainly lipids) during experimental anaerobic lignite biodegradation. The concentrations of *n*-alkanes, *n*-alkanols, *n*-alkanoic acids, diterpenoids, triterpenoids and steroids present in non-biodegraded samples decreased significantly (in case of some compounds to zero) during biodegradation (Tables 3 and 4). Interestingly, some compound classes and individual organic compounds increased in concentration during lignite decay. We interpret this phenomenon as the gradual decomposition of polymers including lignin and cellulose present in lignite. In biodegraded lignite we have identified typical lignin building blocks including *p*-coumaric and ferulic acids (De Leeuw and Largeau, 1993; Lam et al., 2001; Lu and Ralph, 1998), and their abundant degradation products like phenylpropanoic and phloretic acids, tyrosol and 2-phenylethanol (Table 4; Fig. 5). These and related lignin-derived compounds, including 4-hydroxybenzoic acid, vanillin and vanillic acid, were found in products of CuO oxidation of Miocene lignite (Stefanova et al., 2004). Grasset et al. (2010) also identified *p*-coumaric acid and other compounds with guaiacyl (vanillyl) units in the humic acids of low rank coal using derivatization followed by a reductive cleavage (DFRC) method (Grasset et al., 2010). *p*-Coumaric acid is a common constituent of *Picea* pollen lignin (Hu et al., 1999); and its dominance with derivatives in biodegraded lignite, together with the occurrence of abietic and dehydroabietic acids, as well as ferruginol, 6,7-dehydroferruginol and sugiol (Table 4), suggest a predominantly gymnosperm origin for the investigated brown coal. However, *p*-coumaryl alcohol is a major constituent of *Sphagnum* moss, which can be an important component of detritic lignite (De Leeuw and Largeau, 1993). The preferential occurrence of *p*-coumaric and ferulic acids, as well as their derivatives formed during biodegradation (Table 4; Fig. 5) could be connected with their relatively labile bonds to lignins or carbohydrates by ester linkages (Hedges and Weliky, 1989). In addition to lignin-specific compounds, the important concentration of acetophenone is notable in biodegraded coal. This compound was obtained by lignin pyrolysis (Erdocia et al., 2014) and degradation (Asina et al., 2017), and is also interpreted here as a lignin degradation product, supporting the substantial changes of the lignin structure by bacterial consortia.

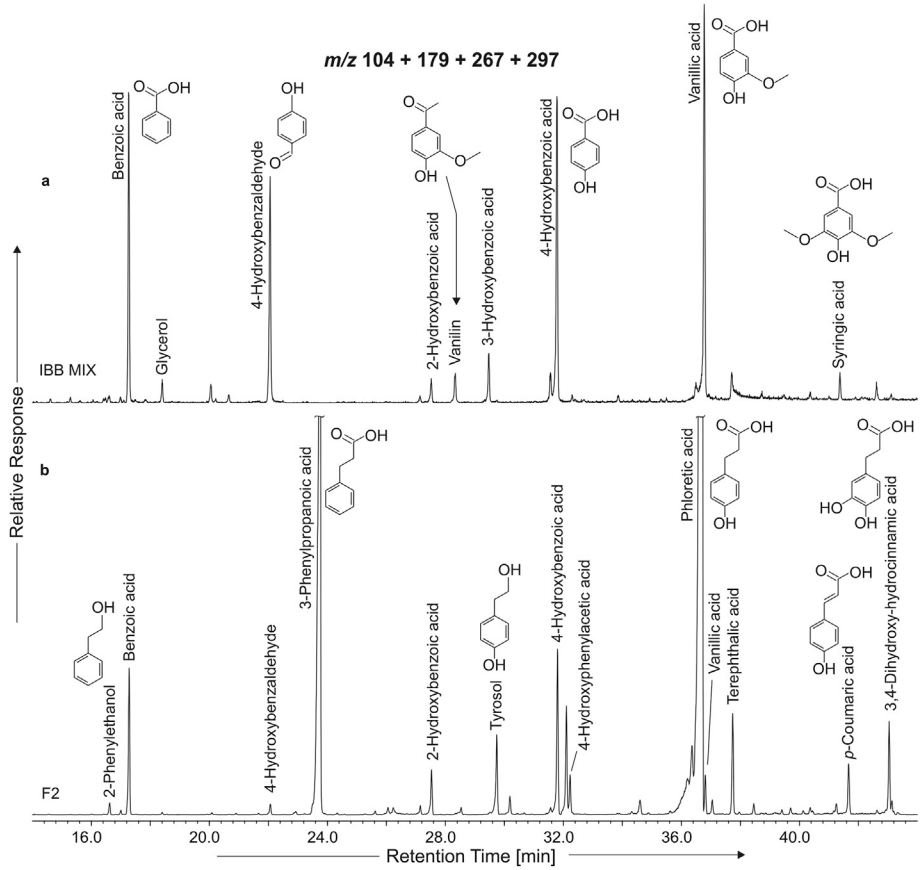

Fig. 5. Summed mass chromatograms (*m/z* 104 + 179 + 267 + 297) showing changes in the lignin degradation product distributions in non-biodegraded (a) and biodegraded (b) lignite. Two main compounds (3-phenylpropanoic acid and phloretic acid) are off-scale to show the smaller peaks in the chromatogram.

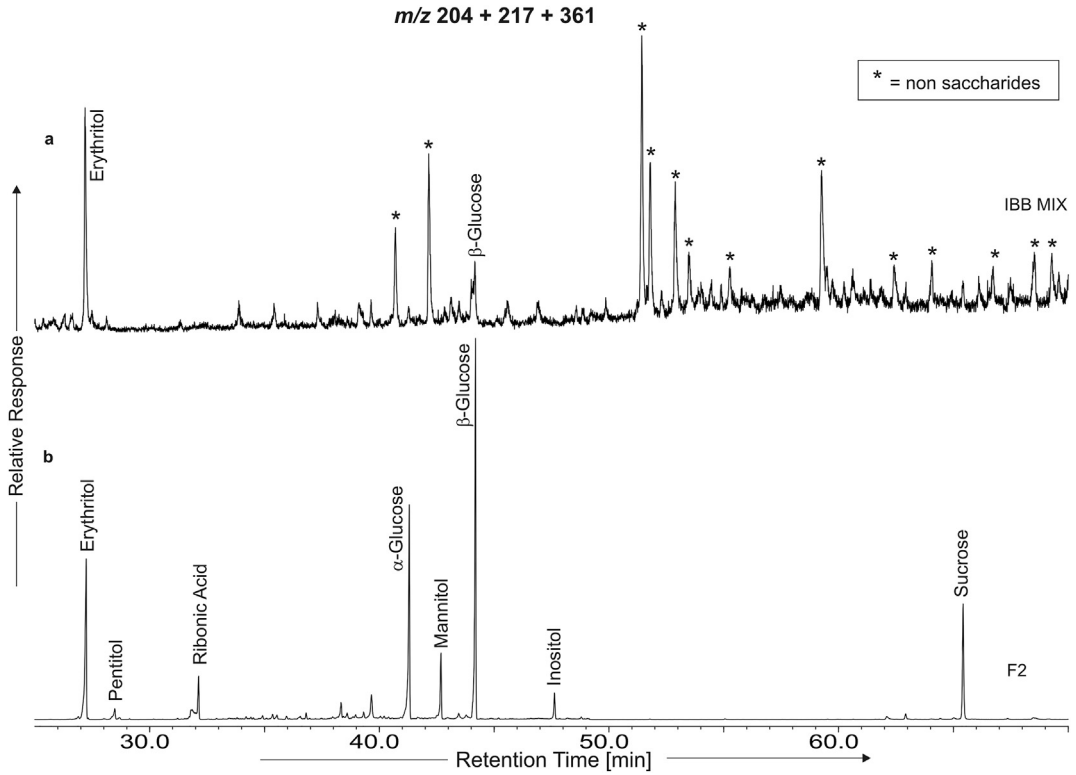

Fig. 6. Summed mass chromatograms (*m/z* 204 + 217 + 361) showing differences in the saccharide concentrations and distributions between non-biodegraded (a) and biodegraded (b) lignite.

Table 5
Biodiversity of the lignite microbial community stimulated by molasses from phylum to genus. *A. major* reads (> 10 reads). *B. minor* reads (< 10 reads).

Phylum	Class	Order: family: genus
A. Major reads		
Firmicutes	*Clostridia*	*Clostridiales: Clostridiaceae: Clostridium, Sarcina; Ruminococcaceae: Ruminococcus: Veillonellaceae: Propionispora; Coriobacteriales: Coriobacteriaceae: Slackia, Atopobium*
	Bacilli	*Lactobacillales: Lactobacillaceae: Lactobacillus, Pediococcus; Carnobacteriaceae: Trichococcus; Streptococcaceae: Lactococcus, Streptococcus; Enterococcaceae: Enterococcus, Tetragenococcus, Vagococcus; Leuconostocaceae: Leuconostoc, Fructobacillus* *Bacillales: Sporolactobacillaceae: Sporolactobacillus; Planococcaceae: Sporosarcina; Bacillaceae: Bacillus, Virgibacillus; Paenibacillaceae: Cohnella* *Exiguobacterales: Exiguobacteraceae: Exiguobacterium*
Bacteroidetes	*Bacteroidia*	*Bacteroidales: Prevotellaceae: Prevotella*; *Bacteroidaceae: Bacteroides*
	Sphingobacteriia	*Sphingobacteriales: Sphingobacteriaceae: Sphingobacterium;*
	Flavobacteriia	*Flavobacteriales: Flavobacteriaceae: Polaribacter*
Actinobacteria	*Actinobacteria*	*Bifidobacteriales: Bifidobacteriacea: Bifidobacterium, Alloscardovia; Actinomycetales: Streptomycetaceae: Streptomyces; Pseudonocardiaceae: Prauserella; Micrococcaceae: Arthrobacter*
Proteobacteria	*Gamaproteobacteria*	*Enterobacteriales: Enterobacteriaceae: Escherichia, Serratia, Citrobacter, Kliebsiella, Enterobacter, Erwinia, Yersinia; Aeromonadaceae: Tolumonas; Ferrimonadaceae: Ferrimonas; Moraxellaceae: Acinetobacter; Vibrionaceae: Vibrio; Pseudomonadaceae: Pseudomonas*
B. Minor reads		
Firmicutes	*Bacilli*	*Lactobacillales: Leuconostocaceae: Weissella, Oenococcus; Aerococcaceae: Alkalibacterium; Carnobacteriaceae: Carnobacterium* *Bacillales: Staphylococcaceae: Macrococcus, Jeotgalicoccus, Staphylococcus; Planococcaceae: Viridibacillus, Lysinibacillus, Planomicrobium; Bacillaceae: Marinococcus, Alkalibacillus, Geobacillus, Lentibacillus; Paenibacillaceae: Paenibacillus, Brevibacillus; Listeriaceae: Listeria, Brochothrix; Thermoactinomycetaceae: Planifilum* *Thermicanales: Thermicanaceae: Thermicanus*
	Clostridia	*Clostridiales: Clostridiaceae: Natronincola, Caloramator, Alkaliphilus; Ruminococcaceae: Oscillospira; Peptococcaceae: Desulfotomaculum, Pelotomaculum; Veillonellaceae: Pectinatus, Negativicoccus; Lachnospiraceae: Johnsonella, Blautia; Carboxydocellaceae: Carboxydocella; Syntrophomonadaceae: Syntrophomonas; Peptostreptococcaceae: Filifactor; Peptococcaceae: Desulfotomaculum* *Thermoanaerobacterales: Thermoanaerobacteraceae: Moorella; Caldicellulosiruptoraceae: Caldicellulosiruptor; Halanaerobiales: Halanaerobiaceae: Halanaerobium; Halobacteroidaceae: Acetohalobium; Natranaerobiales: Anaerobrancaceae:Anaerobranca*
Bacteroidetes	*Bacteroidia,*	*Bacteroidales: Porphyromonadaceae: Porphyromonas*
	Sphingobacteriia	*Sphingobacteriales: Chitinophagaceae; Sphingobacteriaceae: Pedobacter, Olivibacter; Flexibacteraceae: Runella*
	Flavobacteriia,	*Flavobacteriales: Flavobacteriaceae: Flavobacterium*
Actinobacteria	*Actinobacteria*	*Actinomycetales: Micromonosporaceae: Micromonospora; Microbacteriaceae: Microbacterium, Agromyces, Leucobacter, Rathayibacter, Salinibacterium; Yaniellaceae: Yaniella; Nocardioidaceae: Aeromicrobium, Rhodococcus, Nocardioides, Kribbella, Nocardia; Glycomycetaceae: Glycomyces; Actinomycetaceae: Actinomyces; Micrococcaceae: Rothia, Micrococcus; Thermomonosporaceae: Actinoallomurus; Pseudonocardiaceae: Saccharopolyspora, Amycolatopsis, Pseudonocardia, Actinomycetospora; Frankiaceae: Frankia; Bogoriellaceae: Georgenia; Corynebacteriaceae: Corynebacterium; Mycobacteriaceae: Mycobacterium; Kineosporiaceae: Kineococcus; Sanguibacteraceae: Sanguibacter; Sporichthyaceae: Sporichthya; Micromonosporaceae: Actinocatenispora; Propionibacteriaceae: Microlunatus; Streptomycetaceae: Kitasatospora;*
	Thermoleophilia	*Solirubrobacterales: Conexibacteraceae: Conexibacter; Solirubrobacteraceae: Solirubrobacter*
	Acidimicrobiia	*Acidimicrobiales: Iamiaceae: Iamia; Acidimicrobiaceae: Ferrimicrobium, Acidimicrobium*
Proteobacteria	*Alphaproteobacteria*	*Rhodospirillales: Acetobacteraceae: Swaminathania, Acetobacter, Gluconobacter; Rhodospirillaceae: Rhodospirillum, Azospirillum, Rhodovibrio, Roseospira; Rickettsiales: Anaplasmataceae: Neorickettsia; Sphingomonadales: Erythrobacteraceae: Erythrobacter; Sphingomonadaceae: Sphingomonas, Sphingobium, Sphingopyxis; Rhizobiales: Xanthobacteraceae: Azorhizobium; Methylocystaceae: Methylosinus; Hyphomicrobiaceae: Rhodoplanes, Hyphomicrobium;* *Caulobacterales: Caulobacteraceae: Phenylobacterium* *Kiloniellales: Kiloniellaceae: Thalassospira* *Rhodobacterales: Hyphomonadaceae: Maricaulis; Rhodobacteraceae: Paracoccus*
	Betaproteobacteria	*Burkholderiales: Comamonadaceae: Polaromonas, Paucibacter, Comamonas; Oxalobacteraceae: Herminiimonas, Janthinobacterium* *Methylophilales: Methylophilaceae: Methylotenera*
	Deltaproteobacteria	*Desulfovibrionales: Desulfovibrionaceae: Desulfovibrio; Desulfonatronumaceae: Desulfonatronum* *Myxococcales: Polyangiaceae: Chondromyces; Myxococcaceae: Anaeromyxobacter; Haliangiaceae: Haliangiumorder; Cystobacteraceae: Cystobacter* *Bdellovibrionales: Bdellovibrionaceae: Bdellovibrio*
	Epsilonproteobacteria	*Campylobacterales: Campylobacteraceae: Campylobacter, Arcobacter*
	Gammaproteobacteria	*Thiotrichales: Thiotrichaceae: Thiothrix;* *Enterobacteriales: Enterobacteriaceae: Morganella, Trabulsiella, Arsenophonus, Candidatus* Blochmannia, *Providencia, Gluconacetobacter, Brenneria* *Chromatiales: Chromatiaceae: Chromatium, Marichromatium; Ectothiorhodospiraceae: Halorhodospira* *Alteromonadales: Alteromonadaceae: Marinobacter; Idiomarinaceae: Pseudidiomarina* *Pseudomonadales: Moraxellaceae: Psychrobacter, Moraxella* *Oceanospirillales: Oceanospirillaceae: Oceanospirillum, Halomonas, Amphritea* *Alteromonadales: Alteromonadaceae: Glaciecola* *Xanthomonadales: Xanthomonadaceae: Lysobacter, Thermomonas; Sinobacteraceae: Steroidobacter*
Gemmatimonadetes	*Gemmatimonadetes*	*Gemmatimonadales: Gemmatimonadaceae: Gemmatimonas*
Chloroflexi	*Anaerolineae*	*Caldilineales: Caldilineaceae: Caldilinea*
	Ktedonobacteria	*Thermogemmatisporales: Thermogemmatisporaceae: Thermogemmatispora*
Cyanobacteria	*Nostocophycideae*	*Nostocales: Nostocaceae: Nostoc, Dolichospermum;* *Stigonematales: Rivulariaceae: Calothrix*
Planctomycetes	*Brocadiae*	*Brocadiales: Brocadiaceae: Candidatus,* Scalindua
	Planctomycetia	*Gemmatales: Isosphaeraceae: Singulisphaera; Gemmataceae: Gemmata*
Verrucomicrobia	*Opitutae*	*Pelagicoccales: Pelagicoccaceae: Pelagicoccus*
	Spartobacteria	*Chthoniobacterales: Chthoniobacteraceae: Chthoniobacter*
Synergistetes	*Synergistia*	*Synergistales: Synergistaceae: Candidatus* Tammella, *Synergistes; Aminiphilaceae: Aminiphilus*

(*continued on next page*)

Table 5 (*continued*)

Phylum	Class	Order: family: genus
Tenericutes	*Mollicutes*	*Mycoplasmatales: Mycoplasmataceae: Mycoplasma*
		Entomoplasmatales: Entomoplasmataceae: Mesoplasma
		Acholeplasmatales: Acholeplasmataceae: Candidatus Phytoplasma
Nitrospirae	*Nitrospira*	*Nitrospirales: Thermodesulfovibrionaceae: Thermodesulfovibrio*
Caldithrix	*Caldithrixae*	*Caldithrixales: Caldithrixaceae: Caldithrix*
Thermi	*Deinococci*	*Deinococcales: Deinococcaceae: Deinococcus*
Spirochaetes	*Spirochaetes*	*Spirochaetales: Spirochaetaceae: Treponema*
Acidobacteria	*Holophagae*	*Holophagales: Holophagaceae: Geothrix*
Chlamydiae	*Chlamydiia*	*Chlamydiales: Waddliaceae: Waddlia*
Chlorobi	*Chlorobia*	*Chlorobiales: Chlorobiaceae: Chlorobaculum*
Thermodesulfobacteria	*Thermodesulfobacteria*	*Thermodesulfobacteriales: Thermodesulfobacteriaceae: Thermodesulfatator*
Fusobacteria	*Fusobacteria*	*Fusobacteriales: Fusobacteriaceae: Fusobacterium*

The second group of compounds occurring only in biodegraded lignite were saccharides (Fig. 6). Their total concentration was relatively low (1.17 μg/g TOC) and they comprised only a few compounds (Table 4). The occurrence of *α*- and *β*-glucose is probably related to the preservation of cellulose in lignite. Bacterial degradation of cellulose produced some glucose which was utilized as a good energy source for microbial metabolism. The origin of the other saccharides is not clear, but all are common constituents of plants and/or microorganisms (Duquesnoy et al., 2008) and would be linked to lignite during diagenesis with subsequent cleavage by bacterial activity. However, the bacterial origin of some saccharols cannot be ruled out.

Considering anaerobic/anoxic conditions favoring molasses fermentation in the bioreactor, lignite degradation resulted from lignocellulolytic activity of bacteria and production of non-enzymatic lignite-solubilizing compounds including chelators and alkaline substances (Sekhohola et al., 2013). The latter can enable the activity of lignocellulolytic bacteria. Since the bioreactor environment is acidic, micro niches with an alkaline or neutral pH cannot be excluded. This is in agreement with the other study, which posted that pH is one of the main factors limiting coal-bed methane formation in a long-time perspective (Szafranek-Nakonieczna et al., 2018).

4.2. Microbial community

All the taxa found in the lignite microbial community in the PBR with molasses stimulation here were detected in other studies of raw samples of lignite and after enrichment procedures (Colosimo et al., 2016) and citations therein). Since acidic conditions inhibit methane production no methanogens were found, in contrast to other studies where enrichment procedures stimulated the development of methanogens.

Two substantial groups were expected in the microbial community: bacteria fermenting molasses and bacteria degrading lignite; however, their simultaneous activity as well as mutual stimulation and synergistic relations should be considered. It was shown that formation of microbial consortia and synergistic interactions among bacteria enhance degradation of lignocellulose. A more complex substrate results in stronger synergistic interactions (Deng, 2016). Thus the discussion focuses on the potential role of specific groups or taxons of bacteria in lignite biodegradation processes observed in the bioreactor in the light of current knowledge. However, considering a complexity of microbial interactions, it is difficult to clearly define a specific role of the particular taxons in the process of lignite degradation. Better understanding of the microbial community activity would be possible using metatranscriptomic analysis (gene expression) or metaproteomic analysis (microbial function). Such approaches are warranted in the future studies.

Lignocellulolytic bacteria are widespread among most bacterial phyla, including the *Actinobacteria, Acidobacteria, Bacteroidetes, Chloroflexi, Firmicutes, Fibrobacteres, Proteobacteria* (*Alpha-, Beta-, Delta-, Gamma-*), *Spirochaetes,Tenericutes, Thermotogae,* and *Verrucomicrobia,* all represented in the microbial community studied here. Cellulose and hemicellulose degradation under anaerobic digestion is much better recognized than lignin degradation. Metagenomic research of lignite-degrading microbial communities revealed presence of genes encoding hemicellulases (xylanases, xylosidases, rhamnosidases, *endo*-mannases, beta-galactosidase) and cellulases (endoglucanases, cellobiohydrolases, cellobiases) (Pandit et al., 2016). The best recognized lignin-depolymerizing enzymes are fungal lignin peroxidases, Mn peroxidases and laccases that process lignin under aerobic conditions (Shrestha et al., 2017). Genes encoding homologues of these enzymes, as well as aromatic compound-degrading genes are found in metagenomes of microbial communities degrading lignocellulosic biomass (Pandit et al., 2016).

Lactic acid bacteria belonging to the phyla *Firmicutes* (class: *Bacilli,* families: *Lactobacillaceae, Sporolactobacillaceae, Streptococcaceae, Leuconostaceae*) and *Actinobacteria* (family *Bifidobacteriaceae*) were the most abundant bacteria in the bioreactor microbial community. It is assumed that these widespread and universal microbes were supplied to the bioreactor with lignite and their growth and development stimulated by molasses. However, their participation in lignite degradation must be also considered. It was found that some of the microorganisms including *Lactobacillus delbrueckii* strongly attacked and changed the structure of carbon (diamond-like) coatings on medical stainless steel surfaces (Kaczorowska et al., 2002). The *Leuconostoc* and *Weisella* genera are also found in coal microbial communities (Jones et al., 2010). In the other study biosolubilization of lignite measured by loss of its weight after inoculation with *Streptococci* was observed (Sharma et al., 1992). The *Bacilli* generally are well-recognized as bacteria contributing to lignite degradation. *Bacillus* sp. Y7 isolated from weathered lignite minerals in China was shown to solubilize Chinese lignite (Jiang et al., 2013), and *Bacillus mycoides* NS1020 degraded the coal from one of the Polish brown coal mines (Romanowska et al., 2015). In both cases more than one third of the lignite was degraded in about two weeks. The solubilization ability of lignite was correlated with an increase in pH, secretion of thermostable active extracellular substances, as well as an increase in aliphatic and decrease in aromatic hydrocarbons.

The *Actinobacteria* can produce biosurfactants that contribute to solubilization and break down of hydrocarbons (Barnhart et al., 2016). The *Streptomyces* and *Arthrobacter*, found in this study, are known as lignite-solubilizing bacteria under aerobic conditions (Moolick et al., 1989; Strandberg and Lewis, 1987; Torzilli and Isbister, 1994). These bacteria recognized as aerobes living in soil are also able to grow under anoxic/anaerobic conditions. The *Streptomyces* have a fermentative metabolism with lactate as a key fermentation product (Borodina et al., 2005). Also some members of the genus *Arthrobacter* gain energy from nitrate reduction to ammonia (*A. nicotianae*, *A. globiformis*) or from mixed acid fermentation (*A. globiformis*) under anaerobic conditions (Eschbach et al., 2003).

There are many studies showing that the *Pseudomonas* species, representatives of the *Gammaproteobacteria,* produce lignite-solubilization biosurfactants, use soluble lignite coal as a carbon/energy source (Fuchtenbusch and Steinbuchel, 1999; Gupta et al., 1990; Machnikowska

et al., 2002; Singh and Tripathi, 2013) and are capable of lignite biodesulfurization (Liu et al., 2017). The additional carbon sources such as sucrose, raffinose, fructose; additional nitrogen sources, chelators and metal ions were reported to enhance biodepolymerization of lignite (Selvi et al., 2009). The *Pseudomonadaceae* generally *co*-metabolize a variety of polyaromatic hydrocarbons including dibenzo-*p*-dioxin, phenanthrene and anthracene (Ghosh et al., 2014). The *Pseudomonas*, although aerobes, can grow under anaerobic conditions, e.g. *P. aeruginosa*, and generate energy through denitrification (Toyofuku et al., 2012).

Bacteria belonging to the classes *Clostridia* and *Gammaproteobacteria*, mainly *Enterobacteriaceae,* numerous among the groups found in the PBR at this study are capable of dark fermentation. Thus, in the present system they are responsible for molasses fermentation to hydrogen, carbon dioxide and non-gaseous products such as acetic, butyric, propionic and lactic acids or ethanol (Chojnacka et al., 2011). On the other hand, these bacteria are known to play an important role in the microbial communities degrading lignite due to their lignocellulolytic activity. The *Clostridium, Bacillus* and *Bacteroides* species are capable to degrade cellulose, hemiceluloses and xylans (Singh et al., 2012). They are components of the microbial community called WBC-2 that has already been reported to have the potential to produce methane from coal (Haider et al., 2014; Jones et al., 2008). Hemicellulolytic *Ruminococcus* and *Caldicellulosiruptor* species (Pandit et al., 2016) were also found in the present study. *Desulfotomaculum* sp. (*Peptococcaceae*) grows on a large variety of aromatic compounds including lignite monomers (Vos et al., 2009). Members of the *Peptococcaceae* generally have been described to be involved in the anaerobic degradation of aromatic compounds under various electron acceptor-reducing conditions and frequently in syntrophic associations (Kuppardt et al., 2014).

The *Bacteroides* species and other *Bacteroidetes* such as the *Sphingobacterium* species are found in environments contaminated with toluene (Kuppardt et al., 2014) and petroleum (Yu et al., 2014), whereas *Flavobacterium* are capable of sulfur removal from thiophene, thus participating in coal biodesulfurization processes (Prayuenyong, 2002).

Representatives of the *Gammaproteobacteria* as *Erwinia* (Zhang et al., 2015), *Enterobacter* (Valero et al., 2014), *Acinetobacter, Vibrio* species (Golovin et al., 1996; Valero et al., 2014) are relatively abundant in the microbial communities of this study. *Acinetobacter baumannii* was shown to participate in microbial biotransformation of coal, as enhanced activity of laccases was observed in aerobic conditions (Cubillos-Hinojosa et al., 2017). The *Acinetobacter* sp. are also recognized as degraders of long chain *n*-alkanes (Throne-Holst et al., 2007). The *Vibrio* species are known for their cellulolytic activities (Ramesh and Venugopalan, 1988; Singh et al., 2012). The *Erythrobacter* and *Paracoccus* species (*Alphaproteobacteria*) found here in this microbial community are recognized lignin-degrading bacteria (Pandit et al., 2016). The *Sphingomonas* strains can degrade a wide array of aromatic compounds present in sedimentary lignite (Fredrickson et al., 1999). The genus *Comamonas* (*Betaproteobacteria*) is regarded as a versatile aromatic degrader for phenolics, polycyclic aromatic hydrocarbons and heterocyclic aromatics, such as indole, quinoline and carbazole (Jia et al., 2016).

This and other studies clearly show that lignin degradation occurs under anaerobic conditions; however, so far it is a poorly-recognized process with ambiguities in comparison to aerobic lignin degradation.

5. Conclusions

Lignite is a rich source of various microorganisms. Stimulating autochthonous microflora of lignite by a molasses-containing medium under anaerobic conditions resulted in acidic fermentation of molasses and degradation of lignite. Decomposition of lignin, cellulose and free (non-bound) organic compounds occurred during lignite incubation probably due to the lignocellulolytic activity of bacteria and production of non-enzymatic lignite-solubilizing compounds. Synergistic interactions between various groups of bacteria are assumed and discussed. Concentrations of many aliphatic and polar compounds present in non-biodegraded lignite samples significantly decreased during biodegradation. The ratio lignin:cellulose increased from 11 to 13 in lignite after its decay, which indicates more intense cellulose biodegradation. The identified products of cellulose degradation were *α*- and *β*-glucose. The origin of the other saccharides is not clear, but all are common constituents of biota. Typical lignin degradation were *p*-coumaric acid, ferulic acid and acetophenone after lignite biodegradation. Additionally, further degradation products were phenylpropanoic and phloretic acids, tyrosol and 2-phenylethanol. Both, cellulose and lignin polymeres, which are typical and major constituents of lignite, were degraded by bacteria under anaerobic conditions.

Funding

We acknowledge the support of The National Science Centre, Poland, through grants: DEC-2015/16/S/ST10/00430 (to MB) and 2015/19/B/ST10/00925 (to LM), and The National Centre for Research and Development, Poland, through grant BIOSTRATEG2/297310/13/NCBiR/2016 (to AS).

Acknowledgments

The authors acknowledge the contributions of PAK Kopalnia Węgla Brunatnego Konin SA for allowing access to lignite samples. We also are grateful to the many individuals from this company contributed their time to the field-sampling process.

Appendix A. Supplementary data

Supplementary data to this article can be found online at https://doi.org/10.1016/j.coal.2018.07.015.

References

Asina, F.N.U., Brzonova, I., Kozliak, E., Kubátová, A., Ji, Y., 2017. Microbial treatment of industrial lignin: successes, problems and challenges. Renew. Sust. Energ. Rev. 77, 1179–1205.

Barnhart, E.P., De León, K.B., Ramsay, B.D., Cunningham, A.B., Fields, M.W., 2013. Investigation of coal-associated bacterial and archaeal populations from a diffusive microbial sampler (DMS). Int. J. Coal Geol. 115, 64–70.

Barnhart, E.P., Weeks, E.P., Jones, E.J.P., Ritter, D.J., McIntosh, J.C., Clark, A.C., Ruppert, L.F., Cunningham, A.B., Vinson, D.S., Orem, W., Fields, M.W., 2016. Hydrogeochemistry and coal-associated bacterial populations from a methanogenic coal bed. Int. J. Coal Geol. 162, 14–26.

Bastow, T.P., van Aarssen, B.G.K., Lang, D., 2007. Rapid small-scale separation of saturate, aromatic and polar components in petroleum. Org. Geochem. 38, 1235–1250.

Batstone, D., Jensen, P., 2011. Anaerobic processes. In: Wilderer, P. (Ed.), Treatise on Water Science. Elsevier B.V, Amsterdam, pp. 615–639.

Bechtel, A., Widera, M., Sachsenhofer, R.F., Gratzer, R., Lücke, A., Woszczyk, M., 2007. Biomarker and stable carbon isotope systematics of fossil wood from the second Lusatian lignite seam of the Lubstów deposit (Poland). Org. Geochem. 38, 1850–1864.

Borodina, I., Krabben, P., Nielsen, J., 2005. Genome-scale analysis of Streptomyces coelicolor A3(2) metabolism. Genome Res. 15, 820–829.

Bucha, M., Jędrysek, M.-O., Kufka, D., Pleśniak, Ł., Marynowski, L., Kubiak, K., Błaszczyk, M., 2018. Methanogenic fermentation of lignite with carbon-bearing additives, inferred from stable carbon and hydrogen isotopes. Int. J. Coal Geol. 186, 65–79.

Chojnacka, A., Blaszczyk, M.K., Szczesny, P., Nowak, K., Suminska, M., Tomczyk-Zak, K., Zielenkiewicz, U., Sikora, A., 2011. Comparative analysis of hydrogen-producing bacterial biofilms and granular sludge formed in continuous cultures of fermentative bacteria. Bioresour. Technol. 102, 10057–10064.

Colosimo, F., Thomas, R., Lloyd, J.R., Taylor, K.G., Boothman, C., Smith, A.D., Lord, R., Kalin, R.M., 2016. Biogenic methane in shale gas and coal bed methane: a review of current knowledge and gaps. Int. J. Coal Geol. 165, 106–120.

Cubillos-Hinojosa, J.G., Valero, N., Peralta Castilla, A.D.J., 2017. Effect of a low rank coal inoculated with coal solubilizing bacteria for the rehabilitation of a saline-sodic soil in field conditions. Rev. Facult. Nacional Agron. Medel. 70, 8271–8283.

De Leeuw, J.W., Largeau, C., 1993. A review of macromolecular organic compounds that comprise living organisms and their role in Kerogen, coal, and petroleum formation. In: Engel, M.H., Macko, S.A. (Eds.), Organic Geochemistry: Principles and Applications. Springer US, Boston, MA, pp. 23–72.

Deng, Y., 2016. Lignocellulose as Carbon Source Promotes Bacterial Synergism and Reduces Antagonism, Biological Sciences. The University of Southern Mississippi (The Aquila Digital Community Dissertations).

Duquesnoy, E., Castola, V., Casanova, J., 2008. Identification and quantitative

determination of carbohydrates in ethanolic extracts of two conifers using 13C NMR spectroscopy. Carbohydr. Res. 343, 893–902.
Erdocia, X., Prado, R., Corcuera, M.Á., Labidi, J., 2014. Influence of reaction conditions on lignin hydrothermal treatment. Front. Energy Res. 2.
Eschbach, M., Möbitz, H., Rompf, A., Jahn, D., 2003. Members of the genus Arthrobacter grow anaerobically using nitrate ammonification and fermentative processes: anaerobic adaptation of aerobic bacteria abundant in soil. FEMS Microbiol. Lett. 223, 227–230.
Fabbri, D., Marynowski, L., Fabianska, M.J., Zaton, M., Simoneit, B.R., 2008. Levoglucosan and other cellulose markers in pyrolysates of Miocene lignites: geochemical and environmental implications. Environ. Sci. Technol. 42, 2957–2963.
Fabbri, D., Torri, C., Simoneit, B.R.T., Marynowski, L., Rushdi, A.I., Fabiańska, M.J., 2009. Levoglucosan and other cellulose and lignin markers in emissions from burning of Miocene lignites. Atmos. Environ. 43, 2286–2295.
Fabiańska, M.J., Kurkiewicz, S., 2013. Biomarkers, aromatic hydrocarbons and polar compounds in the Neogene lignites and gangue sediments of the Konin and Turoszów Brown coal basins (Poland). Int. J. Coal Geol. 107, 24–44.
Fredrickson, J.K., Balkwill, D.L., Romine, M.F., Shi, T., 1999. Ecology, physiology, and phylogeny of deep subsurface Sphingomonas sp. J. Ind. Microbiol. Biotechnol. 23, 273–283.
Fuchtenbusch, B., Steinbuchel, A., 1999. Biosynthesis of polyhydroxyalkanoates from low-rank coal liquefaction products by Pseudomonas oleovorans and Rhodococcus ruber. Appl. Microbiol. Biotechnol. 52, 91–95.
Ghosh, S., Jha, P., Vidyarthi, A.S., 2014. Unraveling the microbial interactions in coal organic fermentation for generation of methane — a classical to metagenomic approach. Int. J. Coal Geol. 125, 36–44.
Golovin, Y.G., Shchipko, M.L., Kuznetsov, B.N., Golovina, V.V., Eremina, A.O., 1996. The study of Kansk-Achinsk lignite bioconversion products. Fuel 75, 139–143.
Grasset, L., Vlčková, Z., Kučerík, J., Amblès, A., 2010. Characterization of lignin monomers in low rank coal humic acids using the derivatization/reductive cleavage method. Org. Geochem. 41, 905–909.
Gupta, R.K., Deobald, L.A., Crawford, D.L., 1990. Depolymerization and chemical modification of lignite coal byPseudomonas cepacia strain DLC-07. Appl. Biochem. Biotechnol. 24, 899–911.
Haider, R., Ghauri, M.A., Jones, E.J., Sanfilipo, J.R., 2014. Methane generation potential of Thar lignite samples. Fuel Process. Technol. 126, 309–314.
Hedges, J.I., Weliky, K., 1989. Diagenesis of conifer needles in a coastal marine environment. Geochim. Cosmochim. Acta 53, 2659–2673.
Hofrichter, M., Fakoussa, R., 2001. Microbial degradation and modification of coal. In: Lignin, Humic Substances and Coal. vol. 1. pp. 393–427.
Hu, F.S., Hedges, J.I., Gordon, E.S., Brubaker, L.B., 1999. Lignin biomarkers and pollen in postglacial sediments of an Alaskan lake. Geochim. Cosmochim. Acta 63, 1421–1430.
Huang, Z., Urynowicz, M.A., Colberg, P.J.S., 2013. Stimulation of biogenic methane generation in coal samples following chemical treatment with potassium permanganate. Fuel 111, 813–819.
Jia, S., Han, H., Zhuang, H., Hou, B., 2016. The pollutants removal and bacterial community dynamics relationship within a full-scale British Gas/Lurgi coal gasification wastewater treatment using a novel system. Bioresour. Technol. 200, 103–110.
Jiang, F., Li, Z., Lv, Z., Gao, T., Yang, J., Qin, Z., Yuan, H., 2013. The biosolubilization of lignite by Bacillus sp. Y7 and characterization of the soluble products. Fuel 103, 639–645.
Jones, E.J.P., Voytek, M.A., Warwick, P.D., Corum, M.D., Cohn, A., Bunnell, J.E., Clark, A.C., Orem, W.H., 2008. Bioassay for estimating the biogenic methane-generating potential of coal samples. Int. J. Coal Geol. 76, 138–150.
Jones, E.J.P., Voytek, M.A., Corum, M.D., Orem, W.H., 2010. Stimulation of methane generation from nonproductive coal by addition of nutrients or a microbial consortium. Appl. Environ. Microbiol. 76, 7013–7022.
Kaczorowska, A., Szczesna-Antczak, M., Antczak, T., Bielecki, S., Couvrat, P., Kaczorowski, W., Niedzielski, P., Mitura, S., 2002. An influence of microorganisms on surfaces covered with diamond-like coatings, Proceedings of the IEEE-EMBS special topic conference on molecular. Cell. Tissue Eng. 163–164.
Kuppardt, A., Kleinsteuber, S., Vogt, C., Lüders, T., Harms, H., Chatzinotas, A., 2014. Phylogenetic and functional diversity within toluene-degrading, sulphate-reducing consortia enriched from a contaminated aquifer. Microb. Ecol. 68, 222–234.
Lam, T.B.T., Kadoya, K., Iiyama, K., 2001. Bonding of hydroxycinnamic acids to lignin: ferulic and p-coumaric acids are predominantly linked at the benzyl position of lignin, not the β-position, in grass cell walls. Phytochemistry 57, 987–992.
Li, D., Hendry, P., Faiz, M., 2008. A survey of the microbial populations in some Australian coalbed methane reservoirs. Int. J. Coal Geol. 76, 14–24.
Liu, T., Hou, J.-H., Peng, Y.-L., 2017. Effect of a newly isolated native bacteria, Pseudomonas sp. NP22 on desulfurization of the low-rank lignite. Int. J. Miner. Process. 162, 6–11.
Lu, F., Ralph, J., 1998. The DFRC method for lignin analysis. 2. Monomers from isolated Lignins. J. Agric. Food Chem. 46, 547–552.
Machnikowska, H., Pawelec, K., Podgórska, A., 2002. Microbial degradation of low rank coals. Fuel Process. Technol. 77-78, 17–23.
Marynowski, L., Bucha, M., Smolarek, J., Wendorff, M., Simoneit, B.R.T., 2018. Occurrence and significance of mono-, di- and anhydrosaccharide biomolecules in Mesozoic and Cenozoic lignites and fossil wood. Org. Geochem. 116, 13–22.
Midgley, D.J., Hendry, P., Pinetown, K.L., Fuentes, D., Gong, S., Mitchell, D.L., Faiz, M., 2010. Characterisation of a microbial community associated with a deep, coal seam methane reservoir in the Gippsland Basin, Australia. Int. J. Coal Geol. 82, 232–239.
Miller, J.H., 1972. Experiments in Molecular Genetics. Cold Spring Harbor Laboratory.
Moolick, R.T., Linden, J.C., Karim, M.N., 1989. Biosolubilization of lignite. Appl. Biochem. Biotechnol. 20, 731.
Naseem, A., Tabasum, S., Zia, K.M., Zuber, M., Ali, M., Noreen, A., 2016. Lignin-derivatives based polymers, blends and composites: a review. Int. J. Biol. Macromol. 93, 296–313.
Opara, A., Adams, D.J., Free, M.L., McLennan, J., Hamilton, J., 2012. Microbial production of methane and carbon dioxide from lignite, bituminous coal, and coal waste materials. Int. J. Coal Geol. 96-97, 1–8.
Otto, A., Simoneit, B.R.T., 2001. Chemosystematics and diagenesis of terpenoids in fossil conifer species and sediment from the Eocene Zeitz formation, Saxony, Germany. Geochim. Cosmochim. Acta 65, 3505–3527.
Pandit, P.D., Gulhane, M.K., Khardenavis, A.A., Purohit, H.J., 2016. Mining of hemicellulose and lignin degrading genes from differentially enriched methane producing microbial community. Bioresour. Technol. 216, 923–930.
Penner, T.J., Foght, J.M., Budwill, K., 2010. Microbial diversity of western Canadian subsurface coal beds and methanogenic coal enrichment cultures. Int. J. Coal Geol. 82, 81–93.
Prayuenyong, P., 2002. Coal biodesulfurization processes. Songklanakarin J. Sci. Technol. 24, 493–507.
Ramesh, A., Venugopalan, V.K., 1988. Cellulolytic activity of luminous bacteria. MIRCEN J. Appl. Microbiol. Biotechnol. 4, 227–230.
Ritter, D., Vinson, D., Barnhart, E., Akob, D.M., Fields, M.W., Cunningham, A.B., Orem, W., McIntosh, J.C., 2015. Enhanced microbial coalbed methane generation: a review of research, commercial activity, and remaining challenges. Int. J. Coal Geol. 146, 28–41.
Robbins, S.J., Evans, P.N., Esterle, J.S., Golding, S.D., Tyson, G.W., 2016. The effect of coal rank on biogenic methane potential and microbial composition. Int. J. Coal Geol. 154–155, 205–212.
Romanowska, I., Strzelecki, B., Bielecki, S., 2015. Biosolubilization of polish brown coal by Gordonia alkanivorans S7 and Bacillus mycoides NS1020. Fuel Process. Technol. 131, 430–436.
Sekhohola, L.M., Igbinigie, E.E., Cowan, A.K., 2013. Biological degradation and solubilisation of coal. Biodegradation 24, 305–318.
Selvi, A.V., Banerjee, R., Ram, L.C., Singh, G., 2009. Biodepolymerization studies of low rank Indian coals. World J. Microbiol. Biotechnol. 25, 1713–1720.
Shannon, C.E., 1948. A mathematical theory of communication. At&T Tech. J. 27, 379–423.
Sharma, D., Singh, S., Behera, B., 1992. Biodegradation of Neyveli lignite and Assam coal. Fuel Sci. Technol. Int. 10, 223–242.
Shrestha, S., Fonoll, X., Khanal, S.K., Raskin, L., 2017. Biological strategies for enhanced hydrolysis of lignocellulosic biomass during anaerobic digestion: current status and future perspectives. Bioresour. Technol. 245, 1245–1257.
Singh, D.N., Tripathi, A.K., 2013. Coal induced production of a rhamnolipid biosurfactant by Pseudomonas stutzeri, isolated from the formation water of Jharia coalbed. Bioresour. Technol. 128, 215–221.
Singh, A.L., Singh, P.K., Singh, M.P., 2012. Biomethanization of coal to obtain Clean Coal energy: a review. Energy Explor. Exploit. 30, 837–852.
Stefanova, M., Maman, O., Guillet, B., Disnar, J.R., 2004. Preserved lignin structures in Miocene-aged lignite lithotypes, Bulgaria. Fuel 83, 123–128.
Strandberg, G.W., Lewis, S.N., 1987. Solubilization of coal by an extracellular product fromStreptomyces setonii 75Vi2. J. Ind. Microbiol. 1, 371–375.
Strąpoć, D., Picardal, F.W., Turich, C., Schaperdoth, I., Macalady, J.L., Lipp, J.S., Lin, Y.S., Ertefai, T.F., Schubotz, F., Hinrichs, K.U., Mastalerz, M., Schimmelmann, A., 2008. Methane-producing microbial community in a coal bed of the Illinois basin. Appl. Environ. Microbiol. 74, 2424–2432.
Strąpoć, D., Mastalerz, M., Dawson, K., Macalady, J., Callaghan, A.V., Wawrik, B., Turich, C., Ashby, M., 2011. Biogeochemistry of microbial coal-bed methane. Annu. Rev. Earth Planet. Sci. 39, 617–656.
Szafranek-Nakonieczna, A., Zheng, Y., Słowakiewicz, M., Pytlak, A., Polakowski, C., Kubaczyński, A., Bieganowski, A., Banach, A., Wolińska, A., Stępniewska, Z., 2018. Methanogenic potential of lignites in Poland. Int. J. Coal Geol. 196, 201–210.
Takahashi, S., Tomita, J., Nishioka, K., Hisada, T., Nishijima, M., 2014. Development of a prokaryotic universal primer for simultaneous analysis of Bacteria and archaea using next-generation sequencing. PLoS One 9, e105592.
Tang, Z., Zhai, C., Zou, Q., Qin, L., 2016. Changes to coal pores and fracture development by ultrasonic wave excitation using nuclear magnetic resonance. Fuel 186, 571–578.
Throne-Holst, M., Wentzel, A., Ellingsen, T.E., Kotlar, H.-K., Zotchev, S.B., 2007. Identification of novel genes involved in long-chain n-alkane degradation by Acinetobacter sp. strain DSM 17874. Appl. Environ. Microbiol. 73, 3327–3332.
Torzilli, A.P., Isbister, J.D., 1994. Comparison of coal solubilization by bacteria and fungi. Biodegradation 5, 55–62.
Toyofuku, M., Uchiyama, H., Nomura, N., 2012. Social Behaviours under anaerobic conditions in Pseudomonas aeruginosa. Int. J. Microbiol. 2012, 405191.
Tuomisto, H., 2010. A diversity of beta diversities: straightening up a concept gone awry. Part 2. Quantifying beta diversity and related phenomena. Ecography 33, 23–45.
Valero, N., Gómez, L., Pantoja, M., Ramírez, R., 2014. Production of humic substances through coal-solubilizing bacteria. Braz. J. Microbiol. 45, 911–918.
Vos, P., Boone, D.R., Garrity, G., Castenholz, R.W., Krieg, N.R., 2009. Bergey's Manual of Systematic Bacteriology: Volume 3: The Firmicutes, Second ed. Springer.
Widera, M., 2016. An overview of lithotype associations of Miocene lignite seams exploited in Poland. Geologos 213.
Yu, Y., Zhang, W., Chen, G., Gao, Y., Wang, J., 2014. Preparation of petroleum-degrading bacterial agent and its application in remediation of contaminated soil in Shengli Oil Field, China. Environ. Sci. Pollut. Res. Int. 21, 7929–7937.
Zhang, J., Liang, Y., Pandey, R., Harpalani, S., 2015. Characterizing microbial communities dedicated for conversion of coal to methane in situ and ex situ. Int. J. Coal Geol. 146, 145–154.
Zheng, H., Chen, T., Rudolph, V., Golding, S.D., 2017. Biogenic methane production from Bowen Basin coal waste materials. Int. J. Coal Geol. 169, 22–27.